Journal of Hydroscience and Hydraulic Engineering
Vol. 17, No.2 November, 1999, 127-138

COLD AIR FLOW AND SIMULATION OF SNOW CLOUDS

By

Keisuke Nakayama

Research Associate, Department of Hydraulic Engineering,
Hokkaido University, Sapporo, Japan

Kazuyoshi Hasegawa

Research Associate, Department of Civil Engineering,
Hokkaido University, Sapporo, Japan

and

Mutsuhiro Fujita

Professor, Department of Civil Engineering,
Hokkaido University, Sapporo, Japan

SYNOPSIS

During winter, snow clouds form on cold air fronts that extend from inland to Ishikari Bay. This study attempted to clarify the relationship between snow clouds and cold air flow. To understand the environmental conditions leading to the formation of snow clouds on cold air fronts, the saturation equivalent potential temperature (θe^*), equivalent potential temperature (θe) and potential temperature (θ) were calculated using radiosonde data recorded before and after the formation of the snow clouds. Numerical simulations using the ARPS (Advanced Regional Prediction System), which was developed by the University of Oklahoma, were made to duplicate snow clouds on the cold air front, and the calculated results were consistent with the distributions of radar echoes recorded on Feb 18, 1996.

INTRODUCTION

Around Ishikari Bay, snow clouds associated with cold air flow known as land breezes are frequently observed. These snow clouds, which cause problems such as traffic congestion in Sapporo City, form a few times a year and remain in the center of Ishikari Bay where they produce heavy snowfalls for long periods. The immediate causes of these clouds are low-pressure cells over Ishikari Bay and seasonal winds, the direction of which are between north and north-west. In this case, the cold air flow is not the main cause of the formation of these snow clouds, it only gives cold air and causes mixing on its front (1) (2). Other types of snow clouds, which are

associated with the cold air flow caused by radiative cooling, appear ten or more times a year and do not cause heavy snowfalls. However, these clouds produce localized snowfalls that cause social problems, such as traffic jams (3). The cold air flow that causes the formation of snow clouds locally, was identified by us, using a kite balloon and other observations, and by analyzing the shape of the cold air flow numerically (4).

In our studies, we showed the height of the cold air flow to be less than 100 m. Numerical computation using a two-layered flow assumption in which by us cold air density heavier than the upper air density was assumed, the temperature on the interface rapidly changes vertically and that of the cold air flow layer and the upper flow layer can be separated, also showed that the height of the cold air flow was about 60 m (5). This means that the height of the cold air flow is very low and whether the formation of snow clouds is due to an ascending wind on the cold air front is uncertain.

The main purpose of previous research on the snow clouds associated with cold air flow was to clarify the mechanism that sustains snow clouds over a long period (2). The results indicated that cold air flow has a great effect on the formation of snow clouds. However, the discussion was limited to a consideration of the cold air flow as an energy budget, and little attention was given to the formation and motion of cold air flow.

This study aimed to clarify the relationship between snow clouds and the state of the atmosphere, and to confirm the appearance of snow clouds when cold air flow extended over Ishikari Bay using the ARPS (Advanced Regional Prediction System) that was developed by the University of Oklahoma.

POTENTIAL TEMPERATURE AND SPECIFIC HUMIDITY BEFORE AND AFTER THE FORMATION OF SNOW CLOUDS

On Feb 18, 1996, snow clouds and cold air flow extended over Ishikari Bay. In this section, we discuss the state of the atmosphere as it existed at that time.

Before the formation of the snow clouds

Radiosonde data are obtained everyday at 9:00 and at 21:00, and the data obtained at 21:00 on Feb 17,1996, was used as the data before the formation of snow clouds that appeared at 6:00 on Feb 18. Figures 1 and 2 show the potential temperature (θ), equivalent potential temperature (θe) and saturation equivalent potential temperature (θe^*) obtained by radiosonde in the center of Sapporo City (point A in Figure 3) on Feb 17 and 18, respectively. The temperature near the surface was lower than that of the upper atmosphere because of the presence of the cold air flow, but, as the initial condition, the temperature near the suface of the sea should be thought of as not being affected by the cold air flow. Thus, the temperature near the surface was extrapolated using the radiosonde data from the upper atmosphere to obtain the temperature before the appearance of the cold air flow. Unprocessed radiosonde data is indicated by broken lines.

The lifting condensation level (LCL) was determined as about 200 m by calculating the dew point, and the level of free convection (LFC) was determined as 700 - 800 m from the data shown in Figure 1. That is to say, if the air mass near the surface rises above the LCL by an ascending wind, it condenses and releases latent

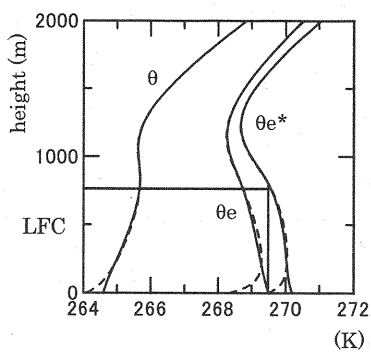

FIGURE 1. Vertical profile of P.T., E.P.T. and S.E.P.T at 21:00 on Feb 17, 1996.

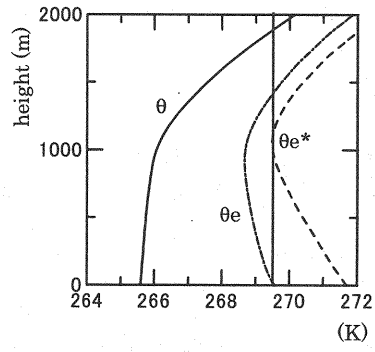

FIGURE 2. Vertical profile of P.T., E.P.T. and S.E.P.T at 9:00 on Feb 18, 1996.

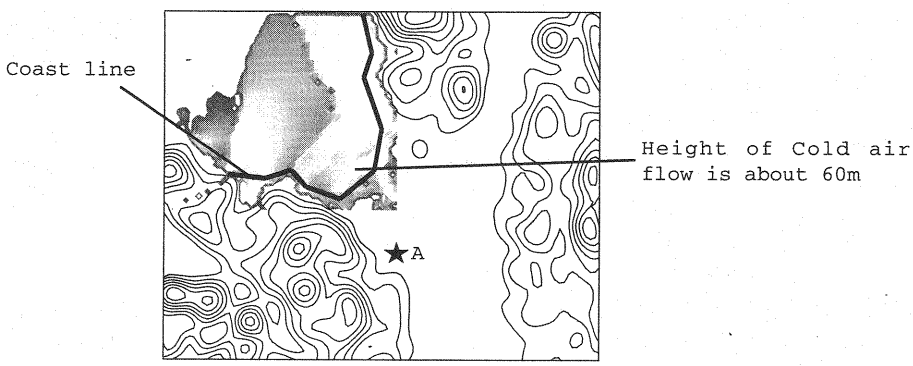

FIGURE 3. Spatial distribution of cold air in the numerical simulation at 6:00 on Feb 18 around Ishikari Bay
(Each contour represents 200m)

heat. Furthermore, if the air mass near the surface rises above the LFC, the temperature of the air mass becomes higher than that of ambient air, which causes the atmosphere to become unstable resulting in cumulus convection.

Before the formation of snow clouds, the LCL was very low and the condensation of vapor could have been caused by only a very small uplifting of surface air. The rising air mass near the surface might result in cumulus convection under the unstable atmospheric conditions that existed at 21:00 on Feb 17.

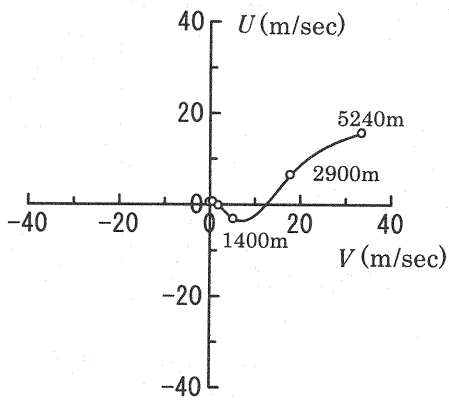

FIGURE 4. Hodograph on Feb 17, 1996.

After the formation of the snow clouds

Figure 2 shows the θ, θe and θe* at 9:00 on Feb 18 after the snow clouds were formed. The LCL was about 650 m, but the LFC was not obtained. This means that the state of the atmosphere was becoming stable due to the reduction of vapor through the formation of the snow clouds and causing cumulus convection under this condition was not possible without the presence of a very strong ascending wind.

NUMERICAL ANALYSIS OF SNOW CLOUDS BY ARPS

Here, we report on our attempts to duplicate snow clouds associated with cold air flow by using the meso-scale meteorological model ARPS. In this model, the wind field is calculated under compression and the non-hydrostatic equilibrium using the turbulent closure model. Cloud microphysical processes were introduced using the method of Tao and Simpson (5).

Initial conditions

Figure 3 shows the height of cold air flow around Ishikari Bay at 6:00 on Feb 18, as obtained by numerical computation (6). The numerical calculation was carried out using a two-layered flow assumption developed by us. The results showed that cold air flow extended over the whole bay area. As the wind direction of the seasonal wind was from the north-west at 18:00 on Feb 17 and from the west at 6:00 on Feb 18, the cold air flow accumulated near the eastern part of Ishikari Bay. Reproducing the cold air flow is impossible using ARPS, because the maximum height of the cold air flow is 60 m and the computation mesh interval has to be less than about 5 m. Therefore, the height of the cold air flow was assumed to be bounded by a rigid boundary (Figure 3). Appendix A gives a detailed explanation of the two-layered flow assumption.

The initial condition of the wind field was determined using radiosonde (Figure 4); where the wind vector in the horizontal plane was given as constant in each vertical mesh point. For the upper, the surface, and the lateral walls, free slip boundary, rigid boundary, and wave-radiation open boundary conditions were imposed, respectively.

The vertical profile of horizontal wind velocities was determined from radiosonde data obtained at 9:00 on Feb 18 because the data changed little between 21:00 on Feb 17 and 9:00 on Feb 18. The vertical profile of potential temperature and specific humidity before and after the formation of the snow clouds corresponded to the conditions observed at 21:00 on Feb 17 and at 9:00 on Feb 18, respectively.

Tao and Simpson's (5) codes are used for cloud microphysical processes, which include clouds, ice, snow and hail. The first-order Large Eddy Simulation model developed by Deardorff (7) is used to calculate the eddy diffusion terms. Because the snow boundary could not be considered as the surface boundary in ARPS, surface fluxes were not included and only the height of the surface was included in the simulation. The important point was to investigate the formation of snow clouds when cold air flow extended over Ishikari Bay. Therefore, to duplicate of the formation of snow clouds, the most important factor was thought to be the shape of the cold air flow. Thus, an assumption without surface fluxes was feasible in this study.

Figure 3 shows the computation area and surface topography. The high frequency components of surface topography are smoothed out. Mesh numbers are 61, 51 (horizontal) and 20 (vertical) and their mesh intervals are 3 km and 3 km (horizontal), while the veritical mesh interval increases from 100 m at the ground/ sea surface to 300 m at the upper wall. The height of the upper wall is given as 4 km. In the northern part of Japan, because the cumulus convection energy is small compared with that of the equator, the height of the snow clouds that occur around Ishikari Bay is lower.

Type 1 (From data obtained before the snow clouds formed)

Figure 5 shows the simulated horizontal distribution of vertical wind velocities near the surface and the snow mixing ratio at 2000 m at 1.0, 1.5 and 2.0 hr after the beginning of the computation. Only snow mixing ratios of greater than 0.01 g/kg are shown to clarify the location of heavy snowfalls. With vertical velocities, the figures show that strong ascending winds at the cold air front were very weak. However the snow mixing ratio indicates that heavy snowfalls were at the cold air front, but not over the mountains. Why the formation of snow clouds at the front can be explained as follows.

The amount of accumulated vapor over the mountainous regions under the LFC was smaller than that over the sea because the LFC was lower (700 - 800 m) and the maximum height of the mountains was 2000 m. Thus, in the first stage of this computation, producing snow clouds over the mountainous region was not easy. Therefore, producing snow clouds over the mountainous region was hard because snow clouds formed at the cold air front and consumed the vapor from Japan Sea,.

The figures at 1.5 hr after the beginning of the computation indicate that the ascending wind and the snow mixing ratio had reached their maximum values. After the maximum snow mixing ratio was attained, snow clouds disappeared. However, in reality, the snow clouds moved in over Sapporo City as they maintain snowfalls. In the simulation, duplicating the mixing at the cold air front was impossible because the effect of the cold air flow was considered as the topography effect only.

Figure 6 shows the snow mixing ratio and vertical wind velocities at 1.5 hr in vertical sections A-A' and B-B' showm in Figure 5. In section B-B', the area of the maximum snow mixing ratio corresponds to the area of the descending winds. In section A-A', ascending winds occur to compensate for the descending winds in section

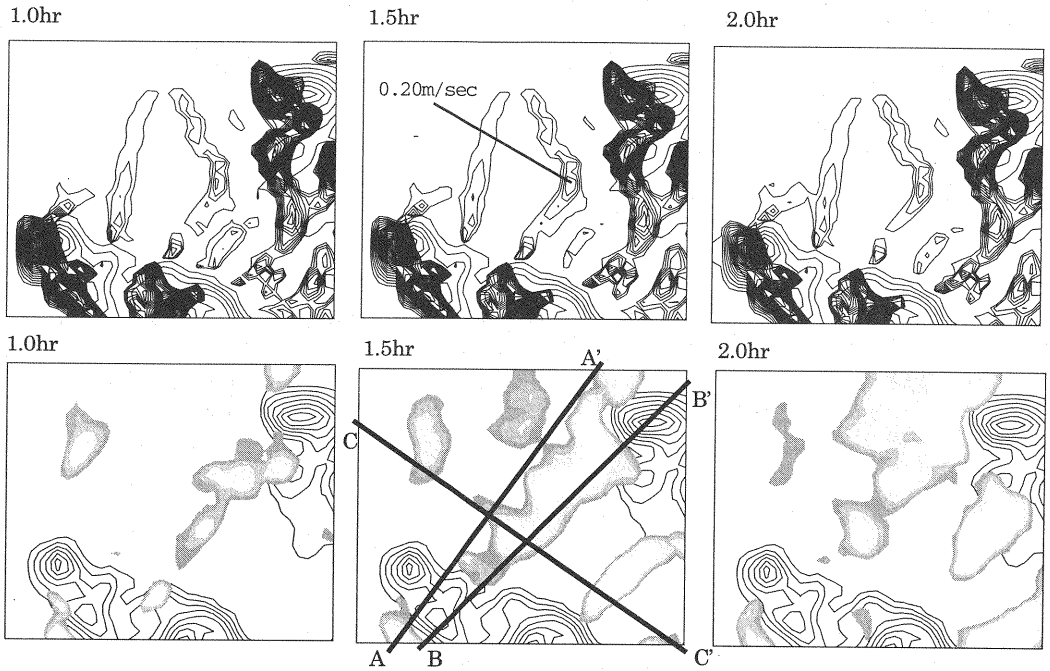

FIGURE 5. Ascending wind near the surface and snow mixing ratio at 2000m at 1.0, 1.5 and 2.0 hr after the beginning of the computation

B-B'. Figure 6 shows that the maximum height of the snow clouds is less than 2 km, while radar observations around Ishikari Bay show that the height of snow clouds is generally less than 4 km in winter.

Figure 7 shows the snow mixing ratios at 0.5, 1.0 and 1.5 hr in section C-C'. In these figures, snow mixing ratios are shown greater than 0.006 g/kg in Figure 6. The direction of the wind was mainly from the left to the right as shown in these figures. At 1.0 hr, snow clouds appeared in the area where the wind velocity was -0.50 m/sec. At 1.5 hr, the snow clouds had increased in size in areas of descending wind.

Type 2 (From data obtained after the snow clouds had formed)

In the simulation in which the initial conditions were given by potential temperature and specific humidity after the formation of the snow clouds, snow clouds appeared over the mountainous region, but not at the cold air front. As was mentioned in the θe^*, θe and θ analysis, snow clouds can not be produced by a weak ascending wind at the cold air front unless a strong ascending wind is applied near the surface. Therefore, this confirms that our analysis is consistent with the numerical simulation results.

Type 3 (From data obtained before the snow clouds formed without a cold air flow)

Figure 8 shows the ascending winds near the surface and snow mixing ratio at 2000 m level at 1.0 hr after the beginning of the computation. Snow clouds did not form in the center of Ishikari Bay because the cold air flow was not considered in the computation. We found that only a little snowfall occurred in the mountainous

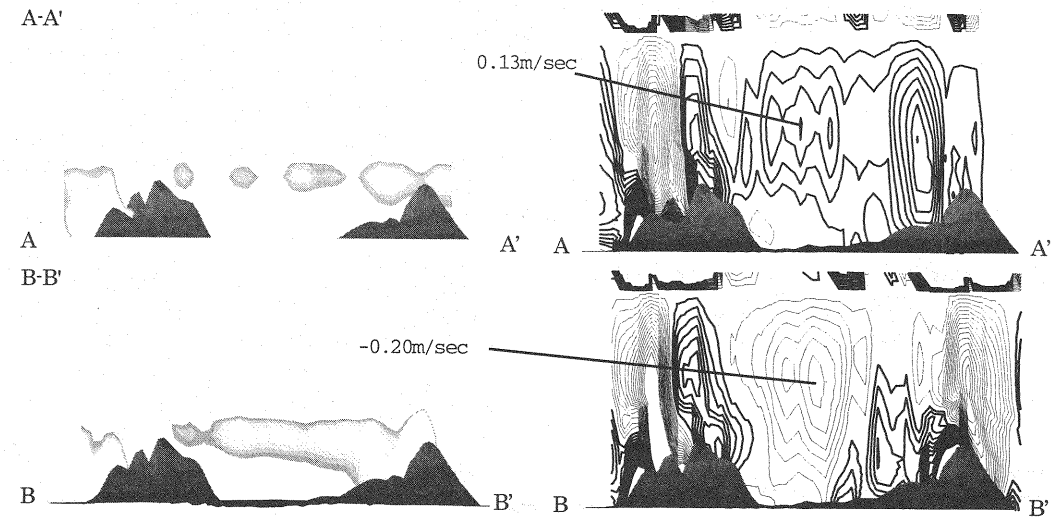

FIGURE 6. Snow mixing ratio (Left) and vertical wind (Right) at 1.5hr in sections A-A' and B-B' (thin and thick solid lines represent descending and ascending winds, respectively)

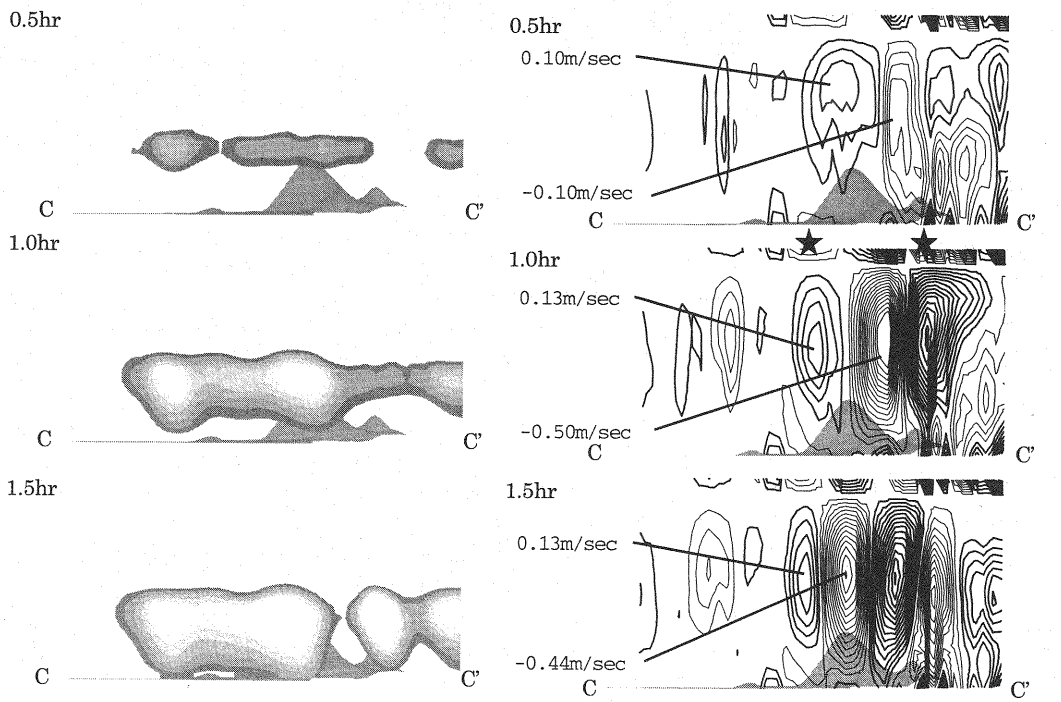

FIGURE 7. Snow mixing ratio (Left) and vertical wind (Right) from 0.5hr to 1.5hr in section C-C' (thin and thick solid lines represent descending and ascending winds, respectively)

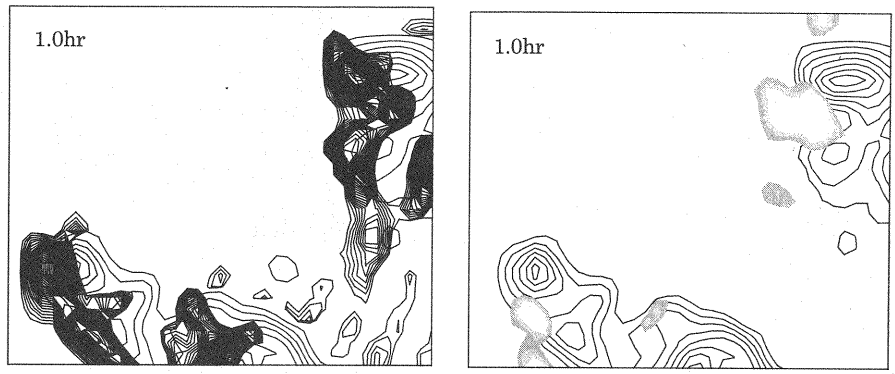

FIGURE 8. Ascending wind near the surface and snow mixing ratio at 2000m at 1.0hr without a cold air flow

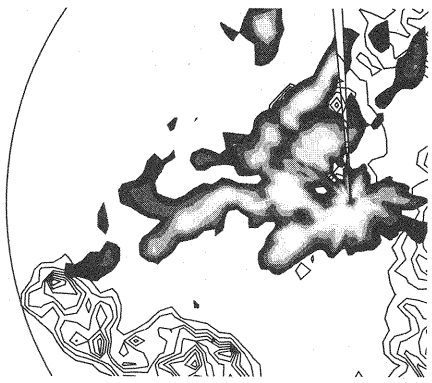

FIGURE 9. Radar intensity around Ishikari Bay at 6:00 on Feb 18

regions. In the following computation, no large values for the snow mixing ratio were noted in Ishikari Bay.

COMPARISON WITH RADAR OBSERVATION

Figure 9 shows horizontal distributions of radar intensity at 6:00 on Feb 18, 1996. This radar intensity occurred suddenly in this area at that time. The value of radar intensity means Bi (=0 - 255, receiving electric power = 112.5+70 Bi/255). The distribution of radar data is bow-shaped because the shape of the cold air front was also bow-shaped. Radar data show large values over a mountain near the center of the radar, but the area of snow clouds is shown smaller than that of the observations. However, the shape of the radar intensity is similar to that of the computation results. Thus, the duplication of the appearance of snow clouds can be said to have been performed successfully.

CONCLUSIONS

(1) By an analysis of θe^*, θe and θ, values for the LCL and LFC were obtained for before and after the formation of the snow clouds.

(2) Ascending wind occurs near the surface due to the cold air front. Therefore ,it is easy to cause snow clouds when a cold air flow occurs over Ishikari Bay.
(3) A comparison of the snow mixing ratio in the numerical simulation and the radar intensity showed good agreement.

REFERENCES

1. Tsuboki, K., Y. Fujiyoshi and G. Wakahama; Structure of a Land Breeze and Snowfall Enhancement at the Leading Edge, Journal of the Meteorological Society of Japan, pp.757-769, 1989.
2. Fujiyoshi, Y., Y. Kodama, K. Tsuboki, K. Nishimura, and N. Ono; Structure of Cold Air During the Development of a Broad Band Cloud and a Meso-scale Vortex; Simultaneous Two-Point Radiosonde Observations, Journal of the Meteorological Society of Japan, Vol.74, pp.281-297, 1996.
3. Nakayama,K., K.Hasegawa and M.Fujita; Structures of Snow Clouds Associated with a Cold Air Flow, Journal of hydraulic, coastal and environmental engineering, No.593, pp.1-10.
4. Nakayama,K., K.Hasegawa and M.Fujita; Analysis of cold air flow with snow cloud in Ishikari bay, Journal of hydraulic, coastal and environmental engineering, No.539, pp.31-42.
5. Tao, W. K., and J. Simpson; Goddard cumulus ensemble model. part 1: Model description, Terrestrial, Atmospheric and Oceanic Sciences, Vol.4, pp.35-72.
6. Nakayama,K., K.Hasegawa and M.Fujita; A Numerical Study on a Cold Air Flow Which Causes Snow Clouds Around Sapporo City, Annual journal of hydraulic engineering, JSCE, Vol.41, pp.129-134.
7. Deardorff,J. : The development of boundary-layer turbulence models for use in studying the severe storm environment, Proc. SESAME Meeting, Boulder, NOAA-ERL, pp.251-264, 1975.
8. Nakayama,K., K.Hasegawa and M.Fujita; A study on the shape of a cold air flow around Ishikari bay in winter at a vertical plane, Annual journal of hydraulic engineering, JSCE, Vol.39, pp.177-182.

Calculation Area :

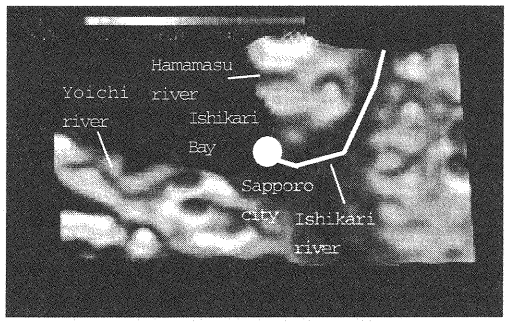

after 4 hours

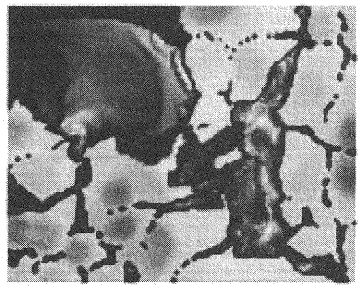

after 8 hours

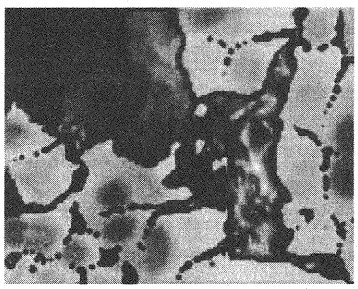

after 12hours

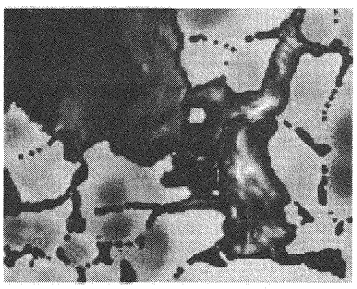

FIGURE A-1.Bird's-eye view of the calculation area
and numerically calculated cold air flow heights from 4 to 12 hours later

Appendix A. Duplication of cold air flow using a two-layered flow assumption

The density of cold air flow is heavier than that of the upper air and the gradient of the temperature on the interface is great. Therefore, cold air flow behaves like a density current because of the buoyancy effect, and the cold air and the upper air flow can be assumed to be a two-layered flow. Equations A-1 to A-3 are the cold air flow model equations. A-1 and A-2 indicate the momentum equations, which include the Coriolis effect (the fourth term on the left), the friction force (the fifth term on the left) and the radiative effect (the second term on the right). A-3 indicates the continuity equation, which includes the generation rate of the cold air.

$$\frac{\partial uh}{\partial t}+\frac{\partial uuh}{\partial x}+\frac{\partial vuh}{\partial y}-fvh+f_i\left(u-U\right)\left|u-U\right|= -\varepsilon gh\frac{\partial h}{\partial x}+\frac{\alpha\left(T-T_T\right)}{\rho_T}gh\frac{\partial h}{\partial x}-\varepsilon gh\frac{\partial Z}{\partial x}+h\nu\nabla^2 u \qquad \text{(A-1)}$$

$$\frac{\partial vh}{\partial t}+\frac{\partial uvh}{\partial x}+\frac{\partial vvh}{\partial y}+fuh+f_i\left(v-V\right)\left|v-V\right|= -\varepsilon gh\frac{\partial h}{\partial y}+\frac{\alpha\left(T-T_T\right)}{\rho_T}gh\frac{\partial h}{\partial y}-\varepsilon gh\frac{\partial Z}{\partial y}+h\nu\nabla^2 v \qquad \text{(A-2)}$$

$$\varepsilon=\frac{\rho_T-\rho}{\rho_T}$$

$$\frac{\partial h}{\partial t}+\frac{\partial uh}{\partial x}+\frac{\partial vh}{\partial y}=R \qquad \text{(A-3)}$$

Here, h is the cold air flow height, u and v are the velocity components in the x and y directions, respectively, f is the Coriolis coefficient, f_i is the friction coefficient of the interface of the two-phase flow, ρ_r is the density of cold air flow, ρ is the density of the upper air, T_r is the temperature of cold air flow, T is the temperature change due to radiative cooling, and R is the intensity of cold air generation.

The numerical simulation was carried out from 18:00 on Feb 17, 1996, to 6:00 on Feb 18, 1996. Figure A-1 shows the calculation area and the results of simulation at 4~12 hours after the onset of radiative cooling. After 4 hours, a cold air flow from the Yoichi and Hamamasu rivers had extended over Ishikari Bay, though the cold air flow from the Hamamasu River was suppressed a little because a seasonal wind was blowing from the west-northwest. After 8 hours, cold air had accumulated around the southern area of the mouth of the Hamamasu River. After 12 hours, cold air had moved south and had made a front, located 20 km from the mouth of the Ishikari River.

The calculations show that the Yoichi and Hamamasu rivers have a great effect on the formation of the cold air flow front, and that cold air is accumulated and strengthened due to the topography of this area.

APPENDIX - NOTATION

The following symbols are used in this paper:

θe^*	= saturation equivalent potential temperature
θe	= equivalent potential temperature
θ	= potential temperature
LCL	= lifting condensation level
LFC	= level of free convection
U	= wind velocity in a westerly wind
V	= wind velocity in a southerly wind
u	= velocity of cold air flow in a westerly wind
v	= velocity of cold air flow in a southerly wind
h	= height of cold air flow
g	= gravity accelaration
Z	= topography height from basic plane
f	= Coriolis coefficient
f_i	= interfacial friction coefficient
ρ_T	= density of cold air flow
ρ	= density of upper air
T_T	= temperature of a cold air flow
T	= temperature which is changed by radiative cooling
ν	= viscosity

(Received October 12, 1998, 1998 ; revised July 5, 1999)